Improved error estimate for extraordinary Catmull-Clark subdivision surface patches

Zhangjin Huang Guoping Wang
Department of Computer Science and Technology
Peking University
Beijing, 100871, China
hzj@graphics.pku.edu.cn

Abstract

Based on an optimal estimate of the convergence rate of the second order norm, an improved error estimate for extraordinary Catmull-Clark subdivision surface (CCSS) patches is proposed. If the valence of the extraordinary vertex of an extraordinary CCSS patch is even, a tighter error bound and, consequently, a more precise subdivision depth for a given error tolerance can be obtained. Furthermore, examples of adaptive subdivision illustrate the practicability of the error estimation approach.

Keywords Catmull-Clark subdivision surfaces, Error estimate, Subdivision depth, Adaptive subdivision

1. Introduction

The Catmull-Clark subdivision surface (CCSS) was designed to generalize the bicubic B-spline surface to the meshes of arbitrary topology [1]. Because a CCSS is defined as the limit of a sequence of recursively subdivided control meshes, the control mesh after several steps of subdivision is often used to approximate the limit surface in applications such as surface rendering, surface trimming, and surface/surface intersection. It is natural to ask the following questions: How to estimate the *error (distance)* between a CCSS and its control mesh? How many (as small as possible) steps of subdivision are needed to satisfy a user-specified error tolerance? Because of the exponential growth in the numbers of mesh faces with successive subdivisions, one more or less step may make a great difference in mesh density. And precise subdivision depth (step) estimation relies on an accurate error estimate.

Optimum distance estimation techniques for regular CCSS patches are available [8, 4]. Distance estimation for an extraordinary CCSS patch is more complicated. Cheng et al. estimated the distance by measuring norms of the *first order differences* of the control points of the given extraordinary CCSS patch [4]. Then they improved the estimate by measuring norms of the *second order differences* of the control points [3]. Furthermore, they introduced a matrix based technique and the two-step convergence rate of second order norms [2]. If the valence of an extraordinary CCSS patch is odd, or even and lower than 8, [2] does give better estimate than [3]. But if the valence is even and higher than 6, [2] may derive improper results (see Table 1) and even worse results than [3] (see Table 2 and Table 3).

The key in Cheng et al.'s approaches [3, 2] is the recurrence formula of the second order norm. Whether their estimate for the convergence rate of the second order norm is optimum for extraordinary CCSS patches? And how can we deal with the extraordinary CCSS patches with high even valences?

In this paper we tackle these problems with an optimization method. The optimal convergence rate of the second order norm can be evaluated by solving constrained minimization problems. Consequently, we find out that Cheng et al.'s estimate for the convergence rate of the second order norm is optimum for odd extraordinary CCSS patches, but not for even ones. And we derive a general error bound formula and show that, for an extraordinary CCSS patch with an extraordinary vertex of even valence, the optimal convergence rate leads to a sharper distance bound and a smaller subdivision depth. As an application, adaptive subdivision is investigated to explain the applicability of our error estimation technique.

2 Definition and notation

Without loss of generality, we assume the initial control mesh has been subdivided at least twice, isolating the extraordinary vertices so that each face is a quadrilateral and contains at most one extraordinary vertex. Then the *valence* of an extraordinary patch is defined as the valence of its only extraordinary vertex.

2.1 Distance between patch and control mesh

Given a control mesh of a Catmull-Clark subdivision surface, for each interior face $\mathbf{F}$, there is a corresponding surface patch $\mathbf{S}$ in the limit surface. $\mathbf{S}$ can be parameterized over the unit square $\Omega = [0,1] \times [0,1]$ as $\mathbf{S}(u,v)$ [9]. Let $\mathbf{F}(u,v)$ be the bilinear parametrization of $\mathbf{F}$ over Ω. For $(u,v) \in \Omega$, we denote by $\|\mathbf{S}(u,v) - \mathbf{F}(u,v)\|$ the distance between the points $\mathbf{S}(u,v)$ and $\mathbf{F}(u,v)$. The *distance* between a CCSS patch $\mathbf{S}$ and the corresponding mesh face $\mathbf{F}$ is defined as the maximum distance between $\mathbf{S}(u,v)$ and $\mathbf{F}(u,v)$ [4], that is,

$$\max_{(u,v)\in\Omega} \|\mathbf{S}(u,v) - \mathbf{F}(u,v)\| \ ,$$

which is also called the distance between the patch $\mathbf{S}$ and the control mesh.

2.2 Second order norm

Let $\Pi = \{\mathbf{P}_i : i = 1, 2, \ldots, 2n+8\}$, be the control mesh of an extraordinary patch $\mathbf{S} = \mathbf{S}_0^0$, with $\mathbf{P}_1$ being the extraordinary vertex of valence n. The control points are ordered following J. Stam's fashion [9] (Figure 1(a)). The *second order norm* of Π, denoted $M = M^0 = M_0^0$, is defined as the maximum norm of the following $2n+10$ *second order differences* (SODs) $\{\alpha_i : i = 1, \ldots, 2n+10\}$ of the control points [3]:

$$\begin{aligned}
M = \max\{ & \{\|\mathbf{P}_{2i} - 2\mathbf{P}_1 + \mathbf{P}_{2((i+1)\%n+1)}\| : 1 \le i \le n\} \\
& \cup \{\|\mathbf{P}_{2i+1} - 2\mathbf{P}_{2(i\%n)+2} + \mathbf{P}_{2(i\%n)+3}\| : 1 \le i \le n\} \\
& \cup \{\|\mathbf{P}_2 - 2\mathbf{P}_3 + \mathbf{P}_{2n+8}\|, \|\mathbf{P}_1 - 2\mathbf{P}_4 + \mathbf{P}_{2n+7}\|, \\
& \quad \|\mathbf{P}_6 - 2\mathbf{P}_5 + \mathbf{P}_{2n+6}\|, \|\mathbf{P}_4 - 2\mathbf{P}_5 + \mathbf{P}_{2n+3}\|, \\
& \quad \|\mathbf{P}_1 - 2\mathbf{P}_6 + \mathbf{P}_{2n+4}\|, \|\mathbf{P}_8 - 2\mathbf{P}_7 + \mathbf{P}_{2n+5}\|, \\
& \quad \|\mathbf{P}_{2n+6} - 2\mathbf{P}_{2n+7} + \mathbf{P}_{2n+8}\|, \\
& \quad \|\mathbf{P}_{2n+2} - 2\mathbf{P}_{2n+6} + \mathbf{P}_{2n+7}\|, \\
& \quad \|\mathbf{P}_{2n+2} - 2\mathbf{P}_{2n+3} + \mathbf{P}_{2n+4}\|, \\
& \quad \|\mathbf{P}_{2n+3} - 2\mathbf{P}_{2n+4} + \mathbf{P}_{2n+5}\|\}\} \\
= \max\{ & \|\alpha_i\| : i = 1, \ldots, 2n+10\} \ .
\end{aligned} \tag{1}$$

By performing a Catmull-Clark subdivision step on Π, one gets $2n+17$ new vertices $\mathbf{P}_i^1, i = 1, \ldots, 2n+17$ (see Figure 1(b)), which are called the *level*-1 *control points* of $\mathbf{S}$. All these level-1 control points compose the *level*-1 *control mesh* of $\mathbf{S}$: $\Pi^1 = \{\mathbf{P}_i^1 : i = 1, 2, \ldots, 2n+17\}$. We use $\mathbf{P}_i^k$ and Π^k to represent the level-k control points and level-k control mesh of $\mathbf{S}$, respectively, after applying k subdivision steps to Π.

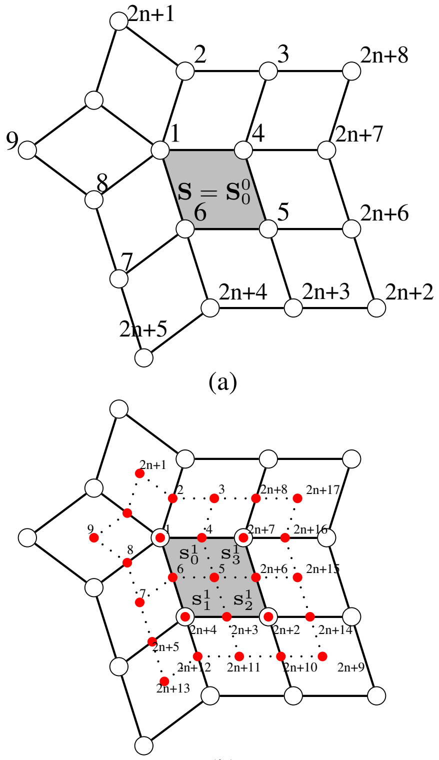

Figure 1. (a) Ordering of control points of an extraordinary patch. (b) Ordering of new control points (solid dots) after a Catmull-Clark subdivision.

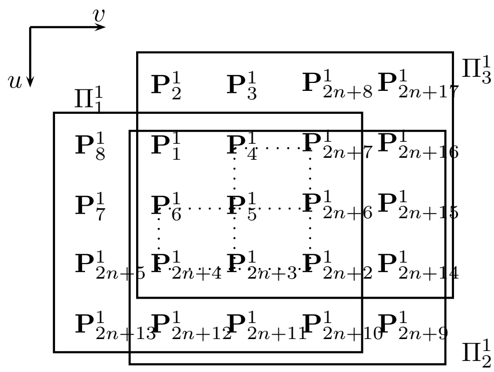

Figure 2. Control points of the subpatches $\mathbf{S}_1^1, \mathbf{S}_2^1$ and $\mathbf{S}_3^1$

The level-1 control points form four control point sets $\Pi_0^1, \Pi_1^1, \Pi_2^1$ and Π_3^1, corresponding to the control meshes of the subpatches $\mathbf{S}_0^1, \mathbf{S}_1^1, \mathbf{S}_2^1$ and $\mathbf{S}_3^1$, respectively (see Figure 1(b)), where $\Pi_0^1 = \{\mathbf{P}_i^1 : 1 \le i \le 2n+8\}$, and the other three control point sets Π_1^1, Π_2^1 and Π_3^1 are shown in Figure 2. $\mathbf{S}_0^1$ is an extraordinary patch, but $\mathbf{S}_1^1$, $\mathbf{S}_2^1$ and $\mathbf{S}_3^1$ are regular patches. Following the notation in Equation (1), one can define the second order norms M_i^1 for $\mathbf{S}_i^1, i = 0, 1, 2, 3$, respectively. $M^1 = \max\{M_i^1 : i = 0, 1, 2, 3\}$ is defined as the second order norm of the level-1 control mesh Π^1. After k steps of subdivision on Π, one gets 4^k control point sets $\Pi_i^k : i = 0, 1, \ldots, 4^k - 1$ corresponding to the 4^k subpatches $\mathbf{S}_i^k : i = 0, 1, \ldots, 4^k - 1$ of $\mathbf{S}$, with $\mathbf{S}_0^k$ being the only level-k extraordinary patch (if $n \neq 4$). We denote by M_i^k and M^k the second order norms of Π_i^k and Π^k, respectively.

3 Recurrence formula of second order norm

The recurrence relation between the second order norms of the control meshes of $\mathbf{S}$ at different subdivision levels is crucial to the error estimation [3, 2]. The second order norms M_0^{k+j} and M_0^j satisfy the following inequality

$$M_0^{k+j} \leq r_j(n) M_0^k, \quad j \geq 0 \ , \tag{2}$$

where $r_j(n)$ is called the *j-step convergence rate* of second order norm, which depends on n, the valence of the extraordinary vertex, and $r_0(n) \equiv 1$.

With a direct decomposition method [3], Cheng et al. gave an estimate of one-step convergence rate $r_1(n)$ as follows:

$$r_1(n) = \begin{cases} \frac{2}{3}, & n = 3 \\ \frac{18}{25}, & n = 5 \\ \frac{3}{4} + \frac{8n-46}{4n^2}, & n > 5 \end{cases} \tag{3}$$

The second order norm of an extraordinary patch $S = S_0^0$ of valence n can be put in the matrix form as follows [2]:

$$M = \|A\mathbf{P}\|_\infty$$

where A is a second order norm matrix of dimension $2n * (2n+1)$

$$A = \begin{bmatrix} -2 & 1 & 0 & 0 & 0 & 1 & 0 & 0 & \cdots & 0 & 0 \\ -2 & 0 & 0 & 1 & 0 & 0 & 0 & 1 & \cdots & 0 & 0 \\ & & & & & \vdots & & & & & \\ -2 & 0 & 0 & 1 & 0 & 0 & 0 & 0 & \cdots & 1 & 0 \\ 0 & -2 & 1 & 0 & 0 & 0 & 0 & 0 & \cdots & 0 & 1 \\ 0 & 0 & 1 & -2 & 1 & 0 & 0 & 0 & \cdots & 0 & 0 \\ & & & & & \vdots & & & & & \\ 0 & 0 & 0 & 0 & 0 & 0 & 0 & 0 & \cdots & -2 & 1 \end{bmatrix}$$

and $\mathbf{P}$ is a control point vector

$$\mathbf{P} = [\mathbf{P}_1, \mathbf{P}_2, \mathbf{P}_3, \ldots, \mathbf{P}_{2n+1}]^T \ .$$

Then the second order norm of the level-k extraordinary subpatch S_0^k can be expressed as:

$$M_0^k = \|A\Lambda^k \mathbf{P}\|_\infty \ ,$$

where Λ is a subdivision matrix of dimension $(2n+1) * (2n+1)$. Cheng et al. proposed an estimate of multi-step convergence rate $r_j(n)$ as follows [2]

$$r_j(n) = \|A\Lambda^j A^+\|_\infty, \quad j \geq 1 \ , \tag{4}$$

where A^+ is the pseudo-inverse matrix of A.

However, it is still unknown whether the estimates (3) and (4) of the convergence rates are optimum for extraordinary CCSS patches. In the following, we derive optimal estimates for $r_j(n), j \geq 1$ by solving constrained minimization problems.

First we estimate $r_1(n)$. Let $\alpha_i^k, i = 1, 2, \ldots, 2n+10$ be the $2n+10$ SODs of $\Pi_0^k, k \geq 0$ defined as in (1). For each $l = 1, 2, \ldots, 2n+10$, we can express α_l^{k+1} as the linear combination of α_i^k:

$$\alpha_l^{k+1} = \sum_{i=1}^{2n+10} x_i^l \alpha_i^k \ ,$$

where $x_i^l, i = 1, 2, \ldots, 2n+10$ are undetermined real coefficients. It follows that

$$\|\alpha_l^{k+1}\| \leq \sum_{i=1}^{2n+10} \|x_i^l \alpha_i^k\| \leq \sum_{i=1}^{2n+10} |x_i^l| \|\alpha_i^k\| \leq \sum_{i=1}^{2n+10} |x_i^l| M_0^k \ .$$

Then we can bound $\|\alpha_l^{k+1}\|$ by $c_l(n) M_0^k$, where $c_l(n)$ is the solution of the following constrained minimization problem

$$\begin{aligned} c_l(n) &= \min \sum_{i=1}^{2n+10} |x_i^l| \ , \\ s.t. \quad & \sum_{i=1}^{2n+10} x_i^l \alpha_i^k = \alpha_l^{k+1} \ . \end{aligned} \tag{5}$$

Since $M_0^{k+1} = \max\{\|\alpha_l^{k+1}\| : 1 \leq l \leq 2n+10\}$, we get an estimate for $r_1(n)$ as follows

$$r_1(n) = \max_{1 \leq l \leq 2n+10} c_l(n) \ .$$

Following the analysis in the complete version of [3], the E-V-E SODs with the extraordinary vertex $\mathbf{P}_1^{k+1}$ as their center points, have the slowest convergence rate. By symmetry, we only need to solve one constrained minimization problem concerned with $\alpha_1^{k+1} = \mathbf{P}_2^{k+1} - 2\mathbf{P}_1^{k+1} + \mathbf{P}_6^{k+1}$. Then it follows that

$$r_1(n) = c_1(n) \ .$$

With the help of the symbolic computation of *Mathematica*, we analyze the values of $c_1(n)$ and obtain the following result on one-step convergence rate. The proof is shown in Appendix B.

Lemma 1 *If M_0^k represents the second order norm of the level-k extraordinary subpatch $S_0^k, k \geq 0$, then*

$$M_0^{k+1} \leq r_1(n) M_0^k \ ,$$

where $r_1(3) = \frac{2}{3}, r_1(5) = \frac{18}{25}$, and

$$r_1(n) = \frac{3}{4} + \frac{2}{n} - \begin{cases} \frac{23}{2n^2}, & \text{if } n \text{ is odd and } n > 5 \\ \frac{16}{n^2}, & \text{if } n \text{ can be divided by } 4 \\ \frac{12}{n^2}, & \text{if } n \text{ is even but can't be divided by } 4 \end{cases}$$

Similarly, we estimate $r_j(n)$ by solving the constrained minimization problem (5) with α_1^{k+1} replaced by α_1^{k+j}. Following from the numerical results (see Table 1), we have

Lemma 2 *If M_0^k represents the second order norm of the level-k extraordinary subpatch $S_0^k, k \geq 0$, then it follows that*

$$M_0^{k+j} \leq r_j(n) M_0^k, \quad j \geq 1 \ ,$$

where

$$r_j(n) \leq \|A\Lambda^j A^+\|_\infty, \quad j \geq 1 \ .$$

Here, equality holds only if n is odd.

The above lemmas work in a more general sense, that is, if M_0^k is replaced with M^k, the second order norm of the level-k control mesh Π^k, the estimates for $r_j(n)$ still work.

Table 1 shows the comparison results of the convergence rates of the second order norm. If the valence n is odd, our estimates equal to the ones of [3, 2]. But if n is even, our technique gives better estimates of the convergence rates. Especially, for one-step convergence rate, if n is even and $n \geq 8$, [2] gives the wrong estimate $r_1(n) > 1$, which conflicts with the basic fact $r_1(n) < 1$.

n	3	5	6	7
$r_1(n)$	0.666667	0.720000	0.750000	0.801020
$r_1(n)[3]$	0.666667	0.720000	0.763889	0.801020
$r_1(n)[2]$	0.666667	0.720000	0.888889	0.801020
$r_2(n)$	0.291667	0.401625	0.468750	0.512117
$r_2(n)[2]$	0.291667	0.401625	0.509838	0.512117
$r_3(n)$	0.122396	0.222541	0.279297	0.314510
$r_3(n)[2]$	0.122396	0.222541	0.287929	0.314510
n	8	10	12	16
$r_1(n)$	0.750000	0.830000	0.805556	0.812500
$r_1(n)[3]$	0.820313	0.835000	0.836806	0.830078
$r_1(n)[2]$	**1.007810**	**1.055000**	**1.229170**	**1.333980**
$r_2(n)$	0.484375	0.559750	0.549190	0.561462
$r_2(n)[2]$	0.569092	0.621375	0.687645	0.732574
$r_3(n)$	0.302734	0.357497	0.360156	0.375187
$r_3(n)[2]$	0.331848	0.376003	0.410135	0.439940

Table 1. Comparison of the convergence rates $r_i(n), \ i = 1, 2, 3$

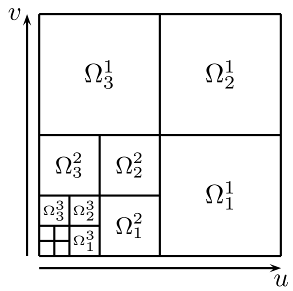

Figure 3. Ω-partition of the unit square.

4 Distance bound

By iteratively performing Catmull-Clark subdivision on $\mathbf{S}$'s extraordinary subpatch, we get a sequence of regular patches $\{\mathbf{S}_b^m\}, m \geq 1, b = 1, 2, 3$, and a sequence of extraordinary patches $\{\mathbf{S}_0^m\}, m \geq 0$. If we use Ω_b^m to represent the parameter space corresponding to $\mathbf{S}_b^m$ then $\{\Omega_b^m\}, m \geq 1, b = 1, 2, 3$, form a partition of the unit square $\Omega = [0, 1] \times [0, 1]$ (see Figure 3) with

$$\begin{aligned} \Omega_1^m &= \left[\frac{1}{2^m}, \frac{1}{2^{m-1}}\right] \times \left[0, \frac{1}{2^m}\right], \\ \Omega_2^m &= \left[\frac{1}{2^m}, \frac{1}{2^{m-1}}\right] \times \left[\frac{1}{2^m}, \frac{1}{2^{m-1}}\right], \\ \Omega_3^m &= \left[0, \frac{1}{2^m}\right] \times \left[\frac{1}{2^m}, \frac{1}{2^{m-1}}\right] \ . \end{aligned}$$

And we denote the parameter space corresponding to the extraordinary subpatch $\mathbf{S}_0^m$ by

$$\Omega_0^m = \left[0, \frac{1}{2^m}\right] \times \left[0, \frac{1}{2^m}\right] \ .$$

The parametrization for $\mathbf{S}(u, v)$ is constructed as follows [9]. For any $(u, v) \neq (0, 0) \in \Omega$, find the Ω_b^m that contains (u, v). m and b can be computed as follows:

$$\begin{aligned} m(u, v) &= \min\left\{\left\lceil \log_{\frac{1}{2}} u \right\rceil, \left\lceil \log_{\frac{1}{2}} v \right\rceil\right\} \\ b(u, v) &= \begin{cases} 1, & \text{if } 2^m u \geq 1 \text{ and } 2^m v \leq 1 \\ 2, & \text{if } 2^m u \geq 1 \text{ and } 2^m v \geq 1 \\ 3, & \text{if } 2^m u \leq 1 \text{ and } 2^m v \geq 1 \end{cases} \end{aligned}$$

The transformation $(u, v) \mapsto (u_m, v_m)$ maps the tile Ω_b^m onto the unit square. Here,

$$t_m = (2^m t)\%1 = \begin{cases} 2^m t, & \text{if } 2^m t \leq 1 \\ 2^m t - 1, & \text{if } 2^m t > 1 \end{cases} , \qquad (6)$$

where t is u or v. Then the value of $\mathbf{S}(u, v)$ is equal to the value of the B-spline patch $\mathbf{S}_b^m$ at (u_m, v_m), i.e.,

$$\mathbf{S}(u,v) = \mathbf{S}_b^m(u_m, v_m) \ .$$

Let $\mathbf{L}(u,v)$, $\mathbf{L}_b^m(u,v)$ and $\mathbf{L}_0^k(u,v)$ be the bilinear parametrization of the center faces of the control meshes of $\mathbf{S}$, $\mathbf{S}_b^m$ and $\mathbf{S}_0^k$, respectively. For $(u,v) \in \Omega_b^m$, the distance between an extraordinary CCSS patch $\mathbf{S}(u,v)$ and the corresponding mesh face $\mathbf{L}(u,v)$ can be bounded as [3]

$$\begin{aligned} \|\mathbf{S}(u,v) - \mathbf{L}(u,v)\| \le\ & \|\mathbf{S}_b^m(u_m,v_m) - \mathbf{L}_b^m(u_m,v_m)\| \\ & + \|\mathbf{L}_b^m(u_m,v_m) - \mathbf{L}_0^{m-1}(u_{m-1},v_{m-1})\| \\ & + \sum_{k=0}^{m-2} \|\mathbf{L}_0^{k+1}(u_{k+1},v_{k+1}) - \mathbf{L}_0^k(u_k,v_k)\| \end{aligned} , \tag{7}$$

where u_m and v_m are defined in (6).

Since $\mathbf{S}_b^m$ is a regular patch, we have [4]

$$\|\mathbf{S}_b^m(u,v) - \mathbf{L}_b^m(u,v)\| \le \frac{1}{3} M_b^m \ , \tag{8}$$

where M_b^m is the second order norm of $\mathbf{S}_b^m$. To estimate the right hand side of (7), we need the following two lemmas.

Lemma 3 *If* $(u,v) \in \Omega_b^m$, $b = 1,2,3$ *then*

$$\left\|\mathbf{L}_b^m(u_m,v_m) - \mathbf{L}_0^{m-1}(u_{m-1},v_{m-1})\right\| \le \frac{1}{4} M_0^{m-1} \ ,$$

where M_0^{m-1} *is the second order norm of* $\mathbf{S}_0^{m-1}$.

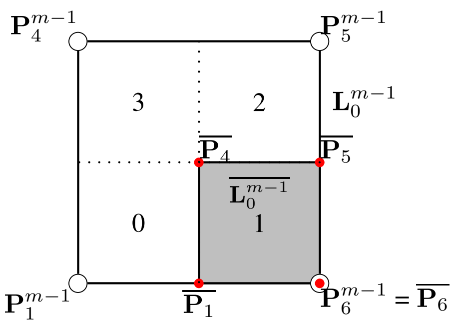

Figure 4. Quarters of $\mathbf{L}_0^{m-1}$

Proof. For the case $b = 1$, if $(u,v) \in \Omega_b^m$, then $(u_{m-1}, v_{m-1}) \in [\frac{1}{2}, 1] \times [0, \frac{1}{2}]$ and $(u_m, v_m) \in [0,1] \times [0,1]$. This means that $\mathbf{L}_0^{m-1}(u_{m-1}, v_{m-1}), (u,v) \in \Omega_1^m$ corresponds to the 1st quarter of $\mathbf{L}_0^{m-1}$ (see Figure 4), i.e.,

$$\begin{aligned} \mathbf{L}_0^{m-1}(u_{m-1},v_{m-1}) =& \overline{\mathbf{L}_0^{m-1}}(u_m,v_m) \\ =& (1-v_m)[(1-u_m)\overline{\mathbf{P}_1} + u_m\overline{\mathbf{P}_6}] \\ & + v_m[(1-u_m)\overline{\mathbf{P}_4} + u_m\overline{\mathbf{P}_5}] \end{aligned} ,$$

where $\overline{\mathbf{P}_1} = \frac{1}{2}(\mathbf{P}_1^{m-1} + \mathbf{P}_6^{m-1})$, $\overline{\mathbf{P}_6} = \mathbf{P}_6^{m-1}$, $\overline{\mathbf{P}_4} = \frac{1}{4}(\mathbf{P}_1^{m-1} + \mathbf{P}_4^{m-1} + \mathbf{P}_5^{m-1} + \mathbf{P}_6^{m-1})$, $\overline{\mathbf{P}_5} = \frac{1}{2}(\mathbf{P}_5^{m-1} + \mathbf{P}_6^{m-1})$.

Referring to Figure 1(b), we have

$$\begin{aligned} \mathbf{L}_1^m(u_m,v_m) =& (1-v_m)[(1-u_m)\mathbf{P}_6^m + u_m\mathbf{P}_{2n+4}^m] \\ & + v_m[(1-u_m)\mathbf{P}_5^m + u_m\mathbf{P}_{2n+3}^m] \end{aligned} .$$

It is easy to know that $\mathbf{P}_5^m = \overline{\mathbf{P}_4}$, i.e., $\|\mathbf{P}_5^m - \overline{\mathbf{P}_4}\| = 0$. And

$$\begin{aligned} & \left\|\mathbf{P}_6^m - \overline{\mathbf{P}_1}\right\| \\ =& \frac{1}{16}\left\|\mathbf{P}_4^{m-1} - 2\mathbf{P}_1^{m-1} + \mathbf{P}_8^{m-1} + \mathbf{P}_5^{m-1} - 2\mathbf{P}_6^{m-1} + \mathbf{P}_7^{m-1}\right\| \\ \le& \frac{1}{8} M_0^{m-1} \ . \end{aligned}$$

Similarly, we get

$$\left\|\mathbf{P}_{2n+3}^m - \overline{\mathbf{P}_5}\right\| \le \frac{1}{8} M_0^{m-1} \ ; \qquad \left\|\mathbf{P}_{2n+4}^m - \overline{\mathbf{P}_6}\right\| \le \frac{1}{4} M_0^{m-1} \ .$$

In fact, we can also solve appropriate constrained minimization problems similar to (5) to obtain the same bound estimates.

Then it follows that

$$\begin{aligned} & \left\|\mathbf{L}_1^m(u_m,v_m) - \mathbf{L}_0^{m-1}(u_{m-1},v_{m-1})\right\| \\ =& \left\|\mathbf{L}_1^m(u_m,v_m) - \overline{\mathbf{L}_0^{m-1}}(u_m,v_m)\right\| \\ \le& \left[\frac{1}{8}(1-v_m)(1-u_m) + \frac{1}{4}(1-v_m)u_m + \frac{1}{8}v_m u_m\right] M_0^{m-1} \ . \end{aligned}$$

By Proposition 1 given in Appendix A, we have

$$\left\|\mathbf{L}_1^m(u_m,v_m) - \mathbf{L}_0^{m-1}(u_{m-1},v_{m-1})\right\| \le \frac{1}{4} M_0^{m-1} \ .$$

For the cases $b = 2$ and $b = 3$, proofs are analogous. ■

Remark 1 *The derivation in [3] has a mistake, which leads to the different bounds for* $b = 2$ *and* $b = 1$ or 3. *Furthermore, our proof is more straightforward and can be easily generalized to other subdivision surfaces such as Doo-Sabin subdivision surfaces [5] and Loop subdivision surfaces [7].*

In analogy to the proof of Lemma 3, we have

Lemma 4 *[3] If* $(u,v) \in \Omega_b^m$, *then for any* $0 \le k < m-1$ *we have*

$$\left\|\mathbf{L}_0^{k+1}(u_{k+1},v_{k+1}) - \mathbf{L}_0^k(u_k,v_k)\right\| \le \frac{1}{\min\{n,8\}} M_0^k \ ,$$

where M_0^k *is the second order norm of* $\mathbf{S}_0^k$ *and* $\mathbf{L}_0^0 = \mathbf{L}$.

By applying Lemma 3, Lemma 4 and (8) on the inequality (7), it follows that if $(u,v) \in \Omega_b^m$,

$$\begin{aligned} &\|\mathbf{S}(u,v) - \mathbf{L}(u,v)\| \\ &\quad \le \frac{1}{3}M_b^m + \frac{1}{4}M_0^{m-1} + \frac{1}{\min\{n,8\}}\sum_{k=0}^{m-2} M_0^k \\ &\quad \le \frac{1}{3}M_b^m + \frac{1}{4}M_0^{m-1} + \frac{1}{\min\{n,8\}}\sum_{k=0}^{m-2} r_k(n)M^0 \end{aligned} \tag{9}$$

Here, $r_k(n)$ is the k-step convergence rate of second order norm.

Since $r_1(n) < 1$ and $r_k(n) \le (r_1(n))^k$, the infinite series $\sum_{k=0}^{\infty} r_k(n) \le \sum_{k=0}^{\infty}(r_1(n))^k = \frac{1}{1-r_1(n)}$. Note that $\lim_{m\to\infty} M_b^m = \lim_{m\to\infty} M_0^{m-1} = 0$. Let $m \to \infty$ in (9), , it follows that

$$\|\mathbf{S}(u,v) - \mathbf{L}(u,v)\| \le \frac{1}{\min\{n,8\}}\sum_{k=0}^{\infty} r_k(n)M^0 \ .$$

Because $\{\Omega_b^m\}, m \ge 1, b = 1,2,3$, form a partition of Ω, we have the following theorem on the maximal distance between $\mathbf{S}(u,v)$ and $\mathbf{L}(u,v)$, $(u,v) \in \Omega$:

Theorem 1 *The distance between an extraordinary CCSS patch* $\mathbf{S}$ *and the corresponding mesh face* $\mathbf{F}$ *is bounded by*

$$\max_{(u,v)\in\Omega} \|\mathbf{S}(u,v) - \mathbf{L}(u,v)\| \le C_\infty(n)M^0 \ ,$$

where

$$C_\infty(n) = \frac{1}{\min\{n,8\}}\sum_{i=0}^{\infty} r_i(n) \ ,$$

and $M^0 = M$ *is the second order norm of* $\mathbf{S}$.

Since there are no explicit expressions for $r_i(n), i > 1$, the above theorem just has theoretical value. Provided that $r_s(n), s = 1,\dots,a$ $(a \ge 1)$ have been computed with the method described in Sect. 3, then for $i = al + j$, $0 \le j \le a-1$, $l \ge 0$, it follows that $r_i(n) \le r_j(n)(r_a(n))^l$. Thus

$$\begin{aligned} \sum_{i=0}^{\infty} r_i(n) &= \sum_{l=0}^{\infty}\sum_{j=0}^{a-1} r_{al+j}(n) \\ &\le \sum_{j=0}^{a-1}\sum_{l=0}^{\infty} r_j(n)(r_a(n))^l = \frac{\sum_{j=0}^{a-1} r_j(n)}{1-r_a(n)} \ . \end{aligned}$$

We get the following practical corollary for error estimation.

Corollary 1 *The distance between an extraordinary CCSS patch* $\mathbf{S}$ *and the corresponding mesh face* $\mathbf{F}$ *is bounded as*

$$\max_{(u,v)\in\Omega} \|\mathbf{S}(u,v) - \mathbf{L}(u,v)\| \le C_a(n)M^0, \quad a \ge 1 \ ,$$

where

$$C_a(n) = \frac{1}{\min\{n,8\}} \frac{\sum_{j=0}^{a-1} r_j(n)}{1-r_a(n)} \ ,$$

and $M^0 = M$ *is the second order norm of* $\mathbf{S}$.

n	3	5	6	7
C_1	1.000000	0.714286	0.666667	0.717947
C_1[3]	1.000000	0.714286	0.705882	0.717949
C_2	0.784314	0.574890	0.549020	0.527357
C_2[2]	0.784314	0.574890	0.642267	0.527357
C_3	0.743818	0.545784	0.513099	0.482061
n	8	10	12	16
C_1	0.500000	0.735294	0.642859	0.666667
C_1[3]	0.695652	0.757576	*0.765957*	*0.735632*
C_2	0.424242	0.519591	0.500642	0.516631
C_2[2]	0.582436	0.678442	**0.892082**	**1.09095**
C_3	0.400560	0.464930	0.460023	0.474935

Table 2. Comparison of $C_a(n)$ $(a = 1,2,3)$

The corollary is a generalization of Lemma 7 in [3] and Lemma 6 in [2], corresponding to the case $a = 1$ and $a = 2$ respectively. But the estimates of $r_j(n)$ may be different from each other. Table 2 gives the comparison results of the bound constants $C_a(n)$ $(a = 1,2,3)$. Because $C_a(n)$ is determined by $r_j(n)$, we draw a similar conclusion as $r_j(n)$: if n is even, our distance bound is sharper than the results of [3, 2]. And if n is quite large such as 12 and 16, [2] may derive an even worse bound than [3].

5 Applications

5.1 Subdivision depth estimation

Because the distance between a level-k control mesh and the surface patch $\mathbf{S}$ is dominated by the distance between the level-k extraordinary subpatch and its corresponding control mesh, which, according to Corollary 1, is

$$\|\mathbf{S}(u,v) - \mathbf{L}^k(u,v)\| \le C_a(n)M^k \ ,$$

where M^k is the second order norm of $\mathbf{S}$'s level-k control mesh. Assume $\epsilon > 0$ and $k = al_j + j, 0 \le j \le a-1$, let

$$\begin{aligned} \|\mathbf{S}(u,v) - \mathbf{L}^k(u,v)\| &\le C_a(n)r_k(n)M^0 \\ &\le C_a(n)(r_a(n))^{l_j} r_j(n)M^0 < \epsilon \ , \end{aligned}$$

then it follows that $l_j \ge \left\lceil \log_{\frac{1}{r_a(n)}}\left(\frac{r_j(n)C_a(n)M^0}{\epsilon}\right)\right\rceil$. Consequently, we have the following subdivision depth estimation formula for extraordinary CCSS patches.

Theorem 2 *Given an extraordinary CCSS patch* $\mathbf{S}$ *and an error tolerance* $\epsilon > 0$*, after*

$$k = \min_{0 \le j \le a-1} al_j + j$$

steps of subdivision on the control mesh of $\mathbf{S}$*, the distance between* $\mathbf{S}$ *and its level-*k *control mesh is smaller than* ϵ*. Here,*

$$l_j = \left\lceil \log_{\frac{1}{r_a(n)}} \left(\frac{r_j(n) C_a(n) M^0}{\epsilon} \right) \right\rceil , \quad 0 \le j \le a-1, a \ge 1 \ ,$$

where $r_j(n)$ *and* $C_a(n)$ *are the same as in Corollary 1,* $M^0 = M$ *is the second order norm of* $\mathbf{S}$*.*

Theorem 2 is also a generalization of Theorem 8 in [3] and Theorem 7 in [2]. Table 3 shows the comparison results of subdivision depths computed by the previous techniques [3, 2] and our approach. Two error tolerances 0.01 and 0.001 are considered and the second order norm M^0 is assumed to be 2. Test results show that the new approach has a 20% improvement over the matrix based technique if n is even. And one can further decrease the depth by increasing the value of a. Note that if n is quite large such as 16 and 20, [2] may give a worse depth estimate than [3].

	$\epsilon = 0.01$				$\epsilon = 0.001$			
n	[3]	[2]	a=2	a=3	[3]	[2]	a=2	a=3
3	14	9	9	8	19	12	12	11
5	16	11	11	10	23	16	16	15
6	19	16	13	12	28	22	19	17
7	23	14	14	12	33	22	22	18
8	26	18	13	12	37	26	19	17
9	27	16	16	14	40	24	24	20
10	28	22	17	14	41	32	24	21
12	29	28	16	14	42	40	24	21
16	*27*	**36**	17	15	*40*	**50**	25	21
20	*26*	**40**	17	15	*37*	**56**	25	22

Table 3. Comparison of subdivision depths

5.2 Adaptive subdivision

In the following, we explain the the practicability of our error estimation approach.

The second order norms of the extraordinary CCSS patches illustrated in Fig. 5 (1a) and (2a) are both 2.83843. Let $a = 3$ and the error tolerance $\epsilon = 0.01$. According to Theorem 2, the subdivision depths are 8 and 12, respectively. This means, if subdivide the control mesh of such an patch uniformly, we need $4^8 = 65,536$ or $4^{12} = 16,777,216$ faces to approximate the limit patch to satisfy the given error precision. Too many faces are required to approximate just one patch. Therefore in such circumstances the uniform subdivision is impractical.

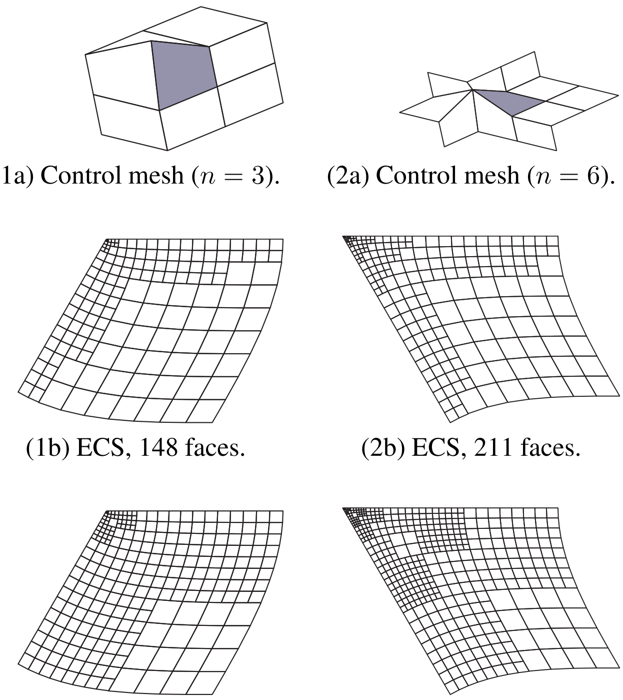

(1a) Control mesh ($n = 3$). (2a) Control mesh ($n = 6$).

(1b) ECS, 148 faces. (2b) ECS, 211 faces.

(1c) DCS, 244 faces. (2c) DCS, 421 faces.

Figure 5. Adaptive subdivision of extraordinary patches.

Notice that after subdivision an extraordinary patch is partitioned into an sequence of regular subpatches and an extraordinary subpatch, and regular patches need much less subdivision steps to satisfy the same precision. For example, the subdivision depth for a regular patch with the second order norm $M = 2.83843$ is 4. Then we can adopt the following two adaptive subdivision strategies:

1. *Error controlled subdivision (ECS)*: Each time before subdividing a (sub)patch, we estimate its error according to Corollary 1. If the error is bigger than the tolerance, perform one step of subdivision; otherwise, stop.

2. *Depth controlled subdivision (DCS)*: First estimate the subdivision depth for each patch of a CCSS according to Theorem 2. For an extraordinary (sub)patch, if its error is smaller than the tolerance, stop; otherwise, perform one step of subdivision and reestimate the subdivision depths of its four subpatches. For a regular (sub)patch, if its subdivision level is equal to the estimated subdivision depth, stop; otherwise perform one step of subdivision.

Figure 5 illustrates examples of adaptive subdivision on two extraordinary CCSS patches, whose valences are 3 and 6 respectively. Fig. 5 (1b) and (2b) are the meshes after error controlled subdivision, while Fig. 5 (1c) and (2c) are the meshes after depth controlled subdivision. The distances (errors) between these approximate meshes and the limit patches are all smaller than $\epsilon = 0.01$. Both the two types of adaptive subdivision achieve significant improvement over uniform subdivision in the number of mesh faces. However, at the cost of relatively more error estimation times, error controlled subdivision performs better than depth controlled subdivision in tessellation and the number of faces.

The examples also show that our error estimate is practical for extraordinary CCSS patches, though the estimated subdivision depths in Table 3 are too large to be applicable at first sight.

6 Conclusions

A new optimization based technique is presented to study the convergence rate of the second order norm of extraordinary CCSS patches. By solving constrained minimization problems, the optimal convergence rates are derived. With a general distance bound formula, improved error estimate for an extraordinary CCSS patch is obtained if the valence of the extraordinary vertex is even. As a result, more precise subdivision depths for a given error tolerance can be obtained. Experiment results show that the new approach improves the matrix based technique [2] by about 20% if the valence is even.

Though, for an extraordinary patch, the slow convergence rate results in a too large subdivision depth to apply uniform subdivision, adaptive subdivision is shown to be effective to produce a high precision approximation.

Given a control mesh of a CCSS, pushing the control points to their limit positions produces a *limit mesh* of the CCSS. In general, a limit mesh approximates the limit surface better than the corresponding control mesh. We explore the distance between a Catmull-Clark subdivision surface and its limit mesh in another paper [6].

Appendix A: a proposition

Proposition 1 *Assume* $a_i \geq 0, i = 0, 1, 2, 3$*, the maximum of the bilinear function* $f(u, v) = (1-v)[(1-u)a_0+ua_1]+v[(1-u)a_2+ua_3]$, $(u, v) \in [0, 1] \times [0, 1]$ *is*

$$\max_{0\leq u,v\leq 1} f(u, v) = \max\{a_0, a_1, a_2, a_3\} \ .$$

Proof. Fix u, then

$$\max_{0\leq v\leq 1} f(u, v) = \max\{(1-u)a_0+ua_1, (1-u)a_2+ua_3\} \ .$$

Since $\max_{0\leq u\leq 1}(1-u)a_0 + ua_1 = \max\{a_0, a_1\}$ and $\max_{0\leq u\leq 1}(1-u)a_2 + ua_3 = \max\{a_2, a_3\}$, we have

$$\max_{0\leq v\leq 1} f(u, v) = \max\{a_0, a_1, a_2, a_3\} \ .$$

This completes the proof. ∎

Appendix B: proof of Lemma 1

Assisted by the symbolic computation of *Mathematica*, we directly have $c_1(3) = \frac{2}{3}, c_1(5) = \frac{18}{25}$.

In the actual computation process, for $\alpha_1^{k+1} = \mathbf{P}_2^{k+1} - 2\mathbf{P}_1^{k+1} + \mathbf{P}_6^{k+1}$, we only need to express it as the linear combination of $2n$ SODs of Π_0^k that involve vertices in the 1-ring of $\mathbf{P}_1^k$, that is, the first $2n$ SODs in (1) :

$$\beta^{k+1} = \sum_{i=1}^{2n} x_i \alpha_i^k \ .$$

Furthermore, by symmetry, there will be only $n + 1$ (if n is odd) or $n + 2$ (if n is even) undetermined coefficients.

Case 1. n is odd and $n > 5$, when $c_1(n)$ is reached, it follows that

$$\begin{aligned}
x_1 &= \frac{1}{2} - \frac{7}{4n^2} \ , \\
x_2 = x_n &= \frac{1}{16} - \frac{7}{4n^2} \ , \\
x_j &= -\frac{7}{4n^2}, \quad j = 3, \ldots, n-1 \ , \\
x_{n+2} = x_{2n} &= \frac{1}{16} - \frac{1}{4n^2} \ , \\
x_{n+j} &= -\frac{1}{4n^2}, \quad j = 1, 3, \ldots, n-1 \ .
\end{aligned}$$

Then

$$c_1(n) = \sum_{i=1}^{2n} |x_i| = \frac{3}{4} + \frac{2}{n} - \frac{23}{2n^2} \ .$$

Case 2. n is even and can be divided by 4, when $c_1(n)$ is reached, it follows that

$$\begin{aligned}
x_1 &= \frac{1}{2} - \frac{4}{n^2} \ , \\
x_{4j-1} &= 0, \quad j = 1, \ldots, \frac{n}{4} \ , \\
x_{4j+1} &= -\frac{4}{n^2}, \quad j = 1, \ldots, \frac{n}{4} - 1 \ , \\
x_2 = x_n &= \frac{1}{16} - \frac{3}{2n^2} \ , \\
x_{2j} &= -\frac{3}{2n^2}, \quad j = 2, \ldots, \frac{n}{2} - 1 \ , \\
x_{n+2} = x_{2n} &= \frac{1}{16} - \frac{1}{2n^2} \ , \\
x_{n+2j} &= -\frac{1}{2n^2}, \quad j = 2, \ldots, \frac{n}{2} - 1 \ , \\
x_{n+2j-1} &= 0, \quad j = 1, \ldots, \frac{n}{2} \ .
\end{aligned}$$

Then

$$c_1(n) = \sum_{i=1}^{2n} |x_i| = \frac{3}{4} + \frac{2}{n} - \frac{16}{n^2} \ .$$

Case 3. n is even and cannot be divided by 4, when $c_1(n)$ is reached, it follows that

$$\begin{aligned}
&x_1 = \frac{1}{2} - \frac{2}{n^2} \ , \\
&x_{2j+1} = -\frac{2}{n^2}, \quad j = 1, \ldots, \frac{n}{2} - 1 \ , \\
&x_2 = x_n = \frac{1}{16} - \frac{3}{2n^2} \ , \\
&x_{2j} = -\frac{3}{2n^2}, \quad j = 2, \ldots, \frac{n}{2} - 1 \ , \\
&x_{n+2} = x_{2n} = \frac{1}{16} - \frac{1}{2n^2} \ , \\
&x_{n+2j} = -\frac{1}{2n^2}, \quad j = 2, \ldots, \frac{n}{2} - 1 \ , \\
&x_{n+2j-1} = 0, \quad j = 1, \ldots, \frac{n}{2} \ .
\end{aligned}$$

Then

$$c_1(n) = \sum_{i=1}^{2n} |x_i| = \frac{3}{4} + \frac{2}{n} - \frac{12}{n^2} \ .$$

This completes the proof.

References

[1] E. Catmull and J. Clark. Recursively generated B-spline surfaces on arbitrary topological meshes. *Computer-Aided Design*, 10(6):350–355, 1978.

[2] G. Chen and F. Cheng. Matrix based subdivision depth computation for extra-ordinary Catmull-Clark subdivision surface patches. In *Proceedings of GMP 2006 (LNCS 4077)*, pages 545–552, 2006.

[3] F. Cheng, G. Chen, and J. Yong. Subdivision depth computation for extra-ordinary Catmull-Clark subdivision surface patches. In *Proceedings of CGI 2006 (LNCS 4035)*, pages 404–416, 2006.

[4] F. Cheng and J. Yong. Subdivision depth computation for Catmull-Clark subdivision surfaces. *Computer Aided Design & Applications*, 3(1–4):485–494, 2006.

[5] D. Doo and M. A. Sabin. Behaviour of recursive subdivision surfaces near extraordinary points. *Computer-Aided Design*, 10(6):356–360, 1978.

[6] Z. Huang and G. Wang. Distance between a Catmull-Clark subdivision surface and its limit mesh. ACM Solid and Physical Modeling Symposium (ACM SPM 2007), accepted, 2007.

[7] C. T. Loop. Smooth subdivision surfaces based on triangles. Master's thesis, Department of Mathematics, University of Utah, August 1987.

[8] D. Lutterkort and J. Peters. Tight linear envelopes for splines. *Numerische Mathematik*, 89(4):735–748, 2001.

[9] J. Stam. Exact evaluation of Catmull-Clark subdivision surfaces at arbitrary parameter values. In *Proceedings of SIGGRAPH 98*, Annual Conference Series, pages 395–404. ACM, 1998.